Field tests for operational shear strength assessment in peat at Uitdam, The Netherlands

C. Zwanenburg
Deltares

Abstract: Stability assessment of existing dikes build on soft soil generates questions on the available stability calculation techniques and material models. Especially peat behaviour is not easily captured by standard design methods. This has led to disapproval, based on calculations, of dikes that have been in operation for several hundreds of years. To establish the weak points in the stability assessment prescribed by the available handbooks on dike engineering, a series of 5 field tests is started. These field tests give the option to compare the different design methods and different parameter assessment techniques to the test results. The series includes single stage and multi stage loading. This paper focuses on the single stage loading tests. The tests result in a failure mode that differs from the circular type failure planes that are used in engineering practice. Horizontal and vertical fractures dominate the active side of the failure while at the passive side the peat is compressed. The tests indicate that tensile strength of peat, or peat fibres, is important in understanding stability problems in which thick peat deposits are involved. Furthermore, the tests show that over-consolidated behaviour is important to understand the measurements, while in engineering practice peat is usually modelled as a normally consolidated material.

Keywords: field tests, peat, shear strength, stability

1 INTRODUCTION

To protect land against flooding a large number of dikes has been erected in The Netherlands since the middle ages. Recently, however, national law obliges local waterboards to prove, with a five-year interval, that water-retaining structures fulfill the required safety level. This led to extensive research programmes for nationwide stability assessment of dikes. For large dike stretches, build on peat layers, the stability assessment results in unexpected low factors of safety. This is explained by the low strength characteristics of peat in combination to the heterogeneity found in laboratory tests and field measurements. Consequently, conservative strength parameters are applied. The question arises if the present day calculation models sufficiently capture the peat behaviour enough for application in stability assessment of existing dikes.

To determine the weak points in the available stability calculation techniques, including the derivation of the required parameters, a series of field tests is started. The field tests focus on peat behaviour. The field tests comprehend forcing a failure plan in a peat layer. Analysis of the test results gives the operational shear strength of this peat layer and is followed by a comparison between the test results and the different calculation techniques including different parameter assessment techniques. The different parameter assessment techniques include the available laboratory tests, e.g. Direct Simple Shear, DSS, triaxial tests etc. but also field measurements, like CPTU, field vane etc.

Full scale testing on real dikes has the disadvantage that a successful tests, the dike is brought to failure, endangers the land that it protects. Full-scale tests on real dikes can only be done in rare occasions. In this study, 5 field tests are planned in which a row of 4 containers is used to model the dike. At the test location, the sub soil contains an approximately 5 m thick peat layer at the top. By using containers, which are remotely filled with water, instead of an earth structure to represent the dike, only

the peat layer contributes to the mobilized shear strength. This makes the assessment of operational shear strength of peat more straight forward.

The five tests represent two types of loading. The first test type comprehends single stage loading; the subsoil is brought to failure directly after erection of the test set-up. The second type comprehends multi stage loading as it includes a consolidation and creep period. Initially a part of the failure load, found in the first test type is applied. After consolidation is finished and some creep has occurred, the load is increased until failure. Two tests of type 1 and three tests of type 2 are planned. Other field tests including single stage and multi stage loading is reported by Lehane & Jardine (2003).

The study started in August 2011 with an extended field survey at the test location. At this moment, the single stage tests are finished while the multi stage tests are now in their consolidation and creep stage. Also, the accompanying laboratory testing programme is not yet completed. This paper discusses only the results of the first test type and the conclusions refer to a part of the study.

The next section discusses the test set-up followed by a characterization of the subsoil in section 3. Some highlights of the field survey and laboratory-testing programme are discussed in section 4 and 5 respectively. Section 6 and 7 discuss the test results so far. Analysis of the measurement data is given by section 8 followed by conclusion in section 9.

2 TEST SET-UP

Figure 1 shows the three phases of the single stage testing procedure. Before the test starts the monitoring equipment is placed followed by the 4 containers as shown by Figure 2. The four containers were not exactly identical. The middle containers (green) had the dimensions, length 7.0 m, width 2.35 m height 2.5 m and empty weight 5500 kg. The containers at both ends (white) had dimensions: length 6.9 m, width 2.25 m, height 2.3 and empty weight 3300 kg. To assure a good alignment of the containers and a clear definition of the basis along which the load is activated on the sub soil, the containers are placed on concrete slabs. The dimensions of the slabs are 2 m × 2 m × 0.14 m and weight 1360 kg.

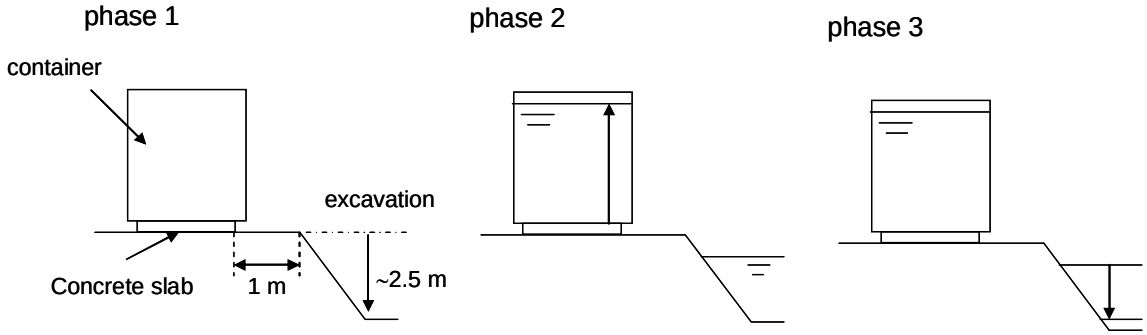

Figure 1. Test procedure.

In phase 1, the excavation is realized. The depth of the excavation is 2.5 m with a 1:1 slope at 1 m distance from the concrete slab. It should be noted that due to swelling the excavation depth reduces during the test.

In phase 2, the loading is activated stepwise by remotely filling the containers with water. Each step raises the water level by 0.25 m. Each next step was made when it was observed that the displacement rates slowed down.

In phase 3, the water table in the excavation was lowered. It should be noted that during excavation the influx of groundwater was small. During phase 2 the water level gradually raised to NAP -1.9 m in test 1 and NAP -2.3 m in test 2. At the end of test 1 the containers tilted considerably. Therefore, the water level inside the containers was maximized at 1.75 m. For test 2 less tilting of the containers was observed. For a comparable result, the filing of the containers in test 2 was stopped at 1.75 m followed by phase 3. No complete failure was found in test 2 after a maximum drawdown of the water table, so extra loading step was applied by filling the containers completely.

a b

Figure 2. Impression of the test facilities a) container row and start excavation b) monitoring equipment.

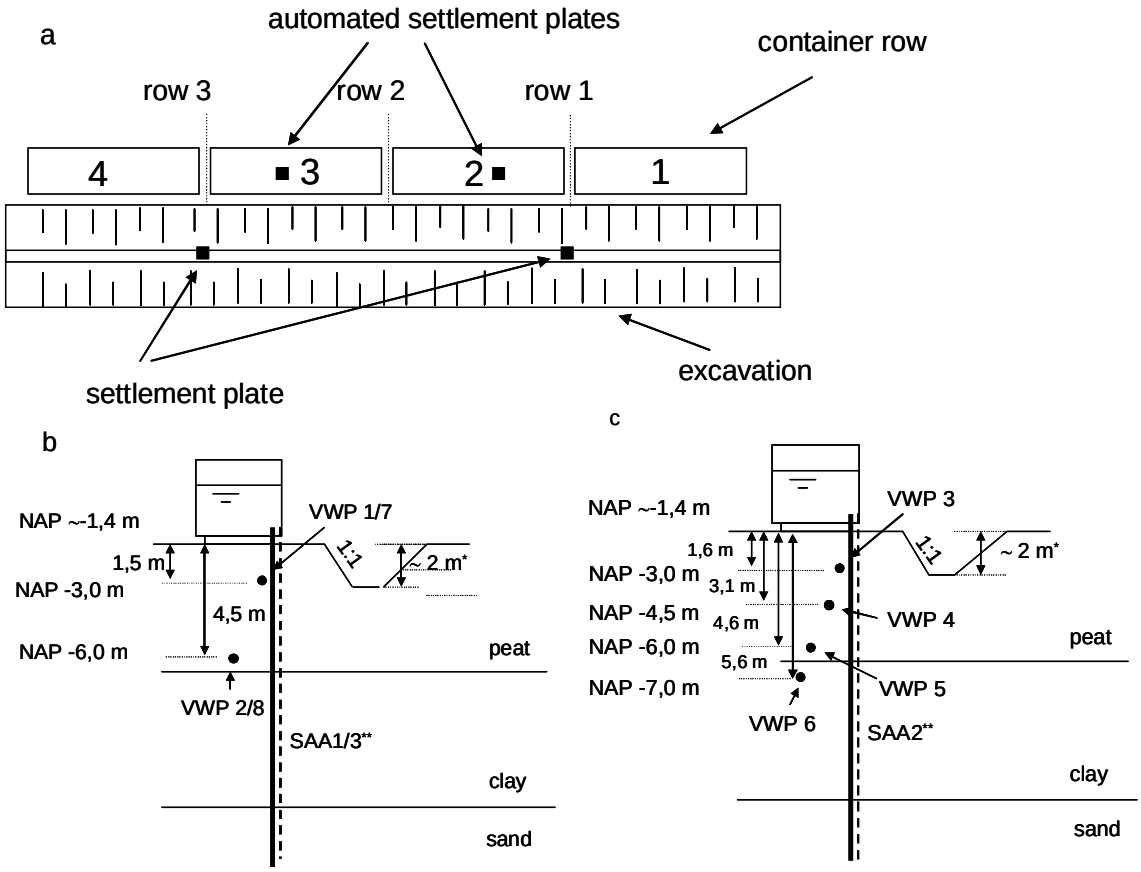

Figure 3. Monitoring a) top view b) cross section row 1 and 3 c) cross section row 2.
* = due to swelling the original depth of 2.5 m was reduced
** = For test 1 SAAs are in line with containers, for test 2 the SAAs are in line with the concrete slabs

The monitoring configuration consists of three measurement rows located between the four containers, see Figure 3a. Each row consists of a Shape Accel Array, SAA, to measure horizontal displacements. Abdoun et al. (2010) give details of this instrument type. Four pore pressure transducers are placed in the middle row and two in the side rows as shown in Figure 3b and 3c. Besides the measurement rows, two automated settlement plates, located under the concrete slabs between measurement row 1 and 2 respectively 2 and 3, measure the vertical displacements. Pressure transducers

are placed in each container to measure the water level. A pressure transducer measures the water table in the excavation and two conventional settlement plates are placed to measure vertical displacements of the excavation. Over a period of approximately 3 months before the tests, the ground water table and the hydraulic head in the pleistocene sand layer. An average ground water table of NAP -1.65 m was found, while the hydraulic head in the pleistocene sand layer was about NAP -2.10 m.

3 SUB SOIL CHARACTERIZATION

Figure 4 shows the location of the test side, approximately 15 km north of Amsterdam along the shores of Lake Markermeer. The area is known for its soft soil conditions. Typically for the area, the ground water table is a few decimeters below ground level. An extended field survey is conducted to characterize the sub soil. Figure 5 shows a typical CPT for the area. Figure 5 presents the depth in relation to reference datum NAP, which is approximately sea level. The sub soil consists of a 0.2 m thick crust followed by a 5 m thick peat layer. The peat layer is followed by sequence of organic and silty clay layers with a total thickness of approximately 5 m. Below the clay layers a thin basal peat layer, with thickness of approximately 0.2 to 0.3 m is present, followed by a thick pleistocene sand layer.

The peat can be described as a sedge-reed peat and is characterized in von Post classification as a H2 to H3 type of peat. This means that the peat is undecomposed (H2) or very slightly decomposed (H3). Plant remains are identifiable and no amorphous material is present. After completion of the test excavation revealed the presence of old horizontal cracks inside the peat layer. These cracks are filled with clay, leading to 1 to 3 mm thick clay layers, known as clay parting. These layers indicate hydraulic fracturing in the past.

Figure 4. Test location

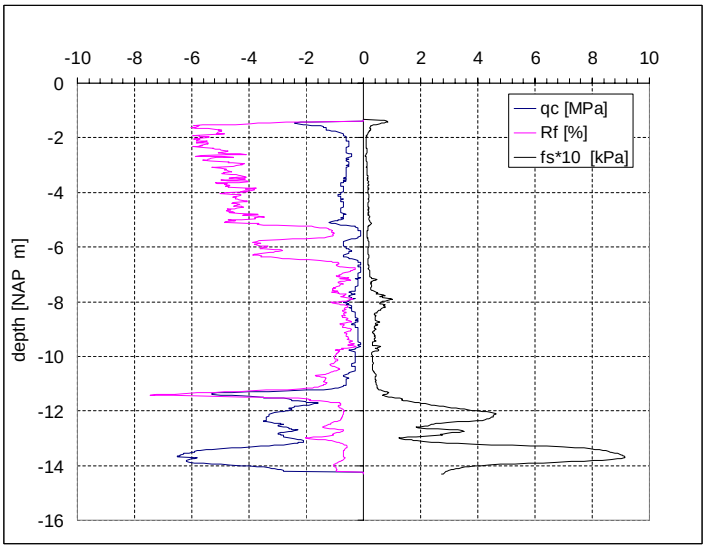

Figure 5. Typical CPT

Figure 6 shows some characteristics of the peat and clay layer below. Figure 6a presents the density, ρ measured in one boring with an interval of 0.2 m. For peat samples densities slightly below the density of water is found. This is explained by loss of some pore water, from larger pores. The increase in density found at the depth of NAP – 6 m resembles the transition between the peat and clay layer. Although a density for peat below the water density seems unrealistic, densities nearly equal to the water density is not uncommon for peat, see e.g. Den Haan & Kruse (2007) and Zwanenburg et al (2012), and corresponds to the high water content shown by Figure 6d. It should be noted that the low peat density in combination to the high ground water table leads to a low effective stress level. Figure 6b shows the loss on ignition, *N*, found from 10 samples. The value for *N* falls within a narrow range of 82% - 92% with one exception when 75% was found. Figure 6c shows the solid density, ρ_s. A clear difference in solid density between the peat and clay layer is found at a depth NAP – 5.5 m. These values are found from samples collected from different borings, explaining the difference in transition between peat and clay found in the Figures 6a, 6c, 6d and 6e. Skempton & Petley (1970) propose the following relation between loss on ignition and solid density:

$$\frac{1}{\rho_s} = \frac{1-1.04(1-N)}{1.4} + \frac{1.04(1-N)}{2.7} \qquad (1)$$

In which ρ_s represents the density in [t/m^3]. The average value for *N* for the results presented in Figure 6b is *N* = 85.7 % (0.857 in equation 1). From equation (1) follows ρ_s = 1.51 t/m^3, which agrees well to the average value for solid density presented by Figure 6c, ρ_s = 1.52 t/m^3.

As part of the laboratory testing programme, 20 oedometer tests were conducted. For two borings samples were selected with an interval of 0.5 m along the top 5 m. Figure 6d shows the pre-consolidation stress, σ_{vy} found in these tests. In the upper part of the peat layer σ_{vy} ranges from 10 to 15 kN/m^2. Figure 6e shows the initial water content, *W* of eodometer samples and the samples of the tests discussed in section 5. Note that the water content is not presented as a percentage. Figure 6e shows that the water content increases in depth, from approximately *W* = 7 at the top to *W* = 11 at the bottom of the peat layer. An organic clay layer with intermediate values for *W* follows the peat layer. In the silty clay layer *W* = 0.6 to 0.8 is found.

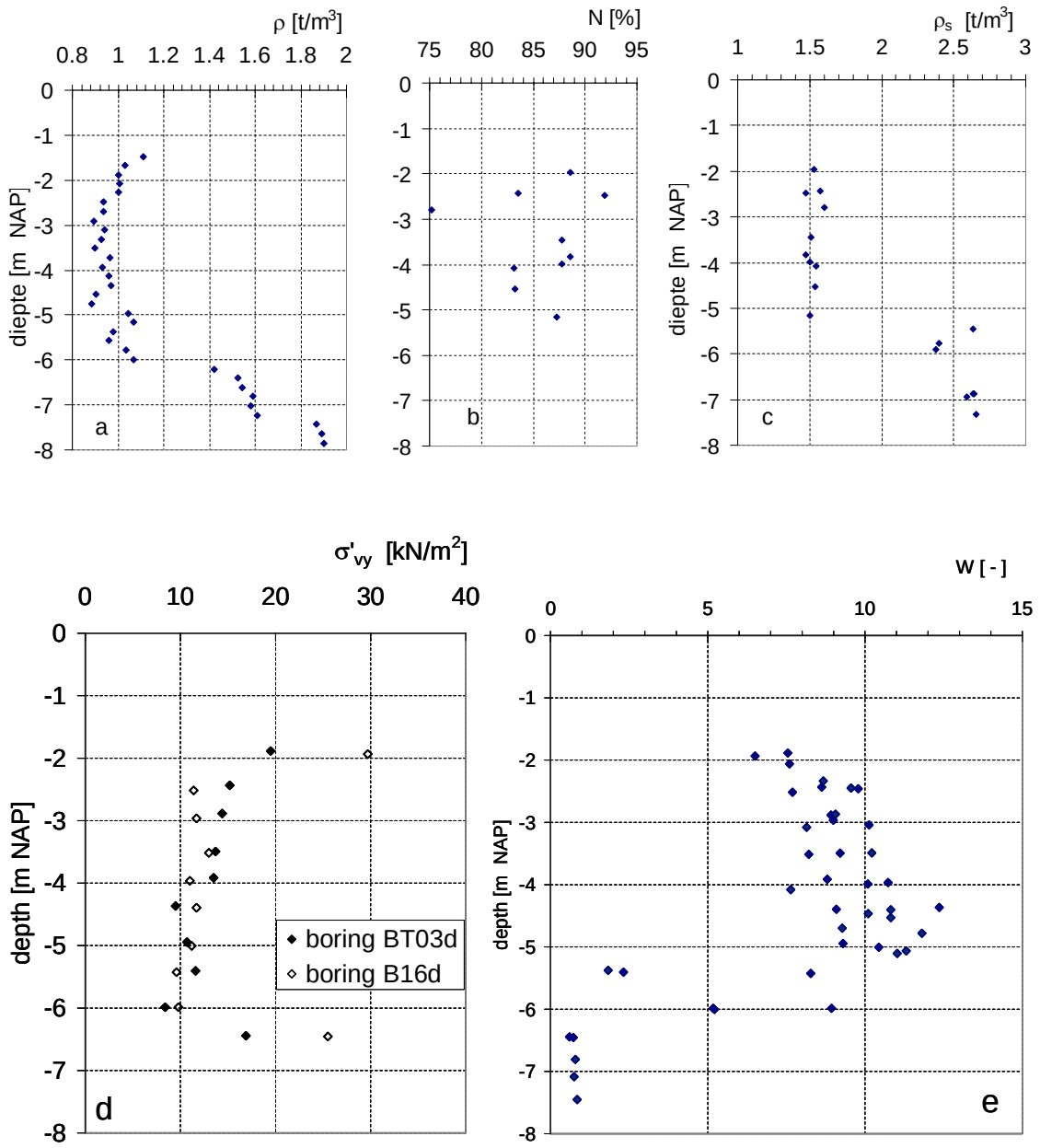

Figure 6. Sub soil characterization, ρ = density [t/m^3], N = loss on ignition [-], ρ_s = solid density [t/m^3], W = water content [-], σ'_{vy} = pre-consolidation stress [kN/m^2]

4 IN-SITU PROBE TESTING

An extended field survey is conducted including CPTU and ball penetrometer tests. This paper discusses a few results. Figure 7 shows the corrected cone resistance, q_t, for 27 conventional CPTU divided over the test area. The corrected cone resistance is defined by:

$$q_t = q_c + (1-a)u_2 \qquad (2)$$

In which q_c represents the cone resistance, a the cone factor and u_2 the pore pressure measured at the shoulder of the cone.

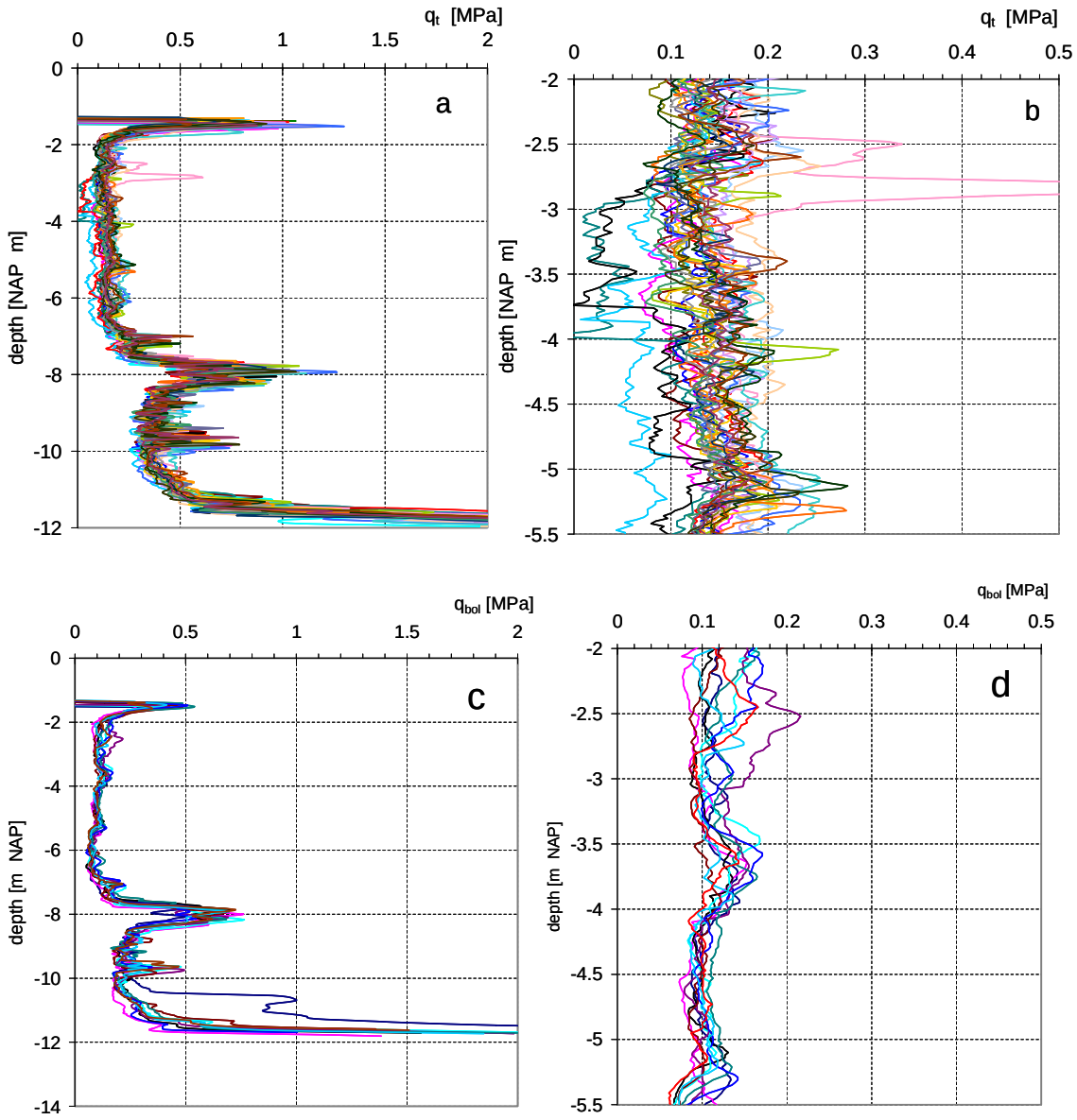

Figure 7. a) corrected resistance for conventional CPTU tests for entire soft soil layer b) zoomed in on peat layer c) ball penetrometer tests for entire soft soil layer d) peat layer

The sub soil shows little variation. The transition between peat and organic clay at approximately NAP -5.5 m to -6 m is not reflected by significant change in q_t. When zoomed in on the peat layer, Figure 7b, q_t, with a few exceptions, falls in a small zone between 0.1 and 0.2 MPa. This is remarkable since peat is known for its heterogeneity. It should be noted that these small values reach the accuracy of conventional CPTU testing.

Figure 7c and 7d show the results of the ball penetrometer tests. The measurements for q_{ball} fall in the same range as q_t, the mean value for q_{ball} = 0.11 MPa and q_t = 0.14 MPa in the peat layer. The difference between both falls with in measurement accuracy. The variation coefficient, V, the ratio of standard deviation and mean value, of q_t is however larger than the variation coefficient of q_{ball}, V_{qt} = 0.21, V_{qball} = 0.17 in the peat layer. The larger dimensions of the ball penetrometer can explain the difference. Since the forces acting on the ball are larger than the forces acting on the standard cone a more accurate reading is possible. Next, the larger volume of the ball makes the measurements less sensitive for small heterogeneities, causing a more constant reading. Due to the smaller variation coefficient the ball penetrometer seems more appropriate for parameter assessment.

Special attention was given to the pore pressure measurement. A special, triple element, cone was applied that measures the pore pressure around the cone at three different levels. Following Lunne et al (1997), these levels are referred to as u_1, u_2 and u_3. Figure 8 depicts the location of the three elements, u_1 in the tip of the cone, u_2 at the shoulder of the cone and u_3 at the top of the friction sleeve.

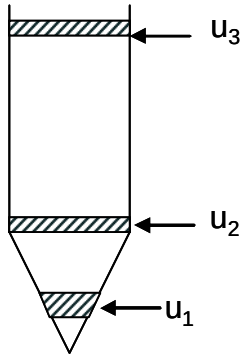

Figure 8. Location of pore pressure measurement along the cone

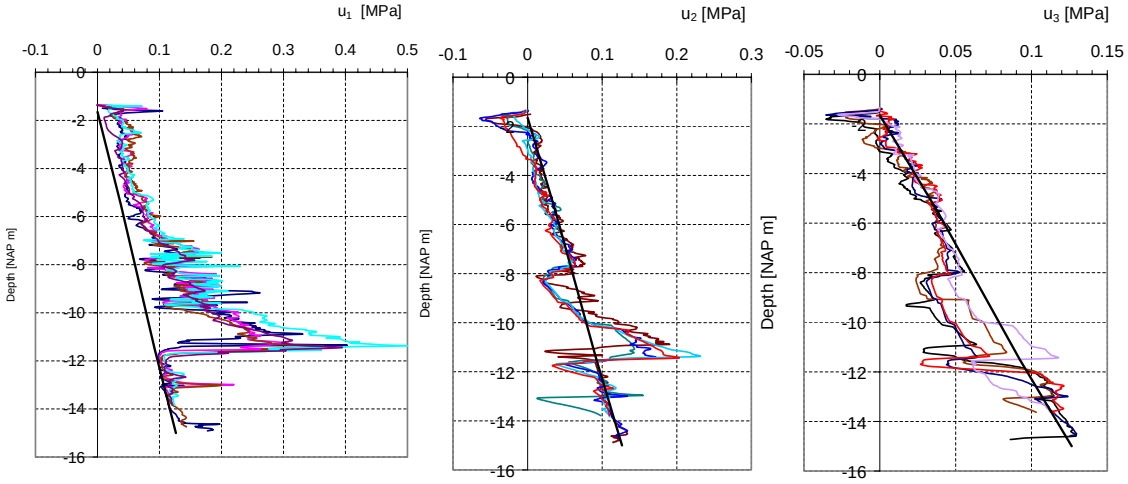

Figure 9. Pore pressure measurements with triple element cone

Figure 9 shows the results, including the hydraulic head, u_0, derived from the measured ground water table and hydraulic head measured in the pleistocene sand layer. The black line in Figure 9 represents u_0. The probe is pushed with a constant rate of 1.5 cm/s. In the peat layer only limited excess pore pressure is found at the u_1 position. In the peat layer, at the u_2 position, the measured pore pressure is nearly equal to the stationary hydraulic head, u_0 or slightly lower. A measured hydraulic head below u_0 indicates an underpressure. Note that in the clay layer below the peat layer at the u_2 position an underpressure was found at approximately NAP - 9 to -10 m followed by an excess pore pressure at NAP -11 to -12 m. At the u_3 position, the stationary head, u_0, is measured in the peat layer. At a lower level, NAP - 9 to -12 m an underpressure is found.

The measurements can be explained by the deformation pattern around the cone, according to Landva (2007). Following an element in the peat layer, when the cone passes, compression of the element is found at the approach of the cone. When the cone enters the soil element, rupture of the fibers occurs and allowing the peat to swell alongside the cone. This swelling causes a reduction of the measured pore pressure. When the cone has passed the soil element, the pore pressure will return to stationary hydraulic head u_o. Each of theses phases are found in the measurements presented by Figure 9. The low excess pore pressure found at the tip of the cone in combination to the near hydrostatic pressure at the shoulder of the cone indicate a relatively high permeability of the peat or large swelling capacity when the peat is unloaded.

The low excess pore pressure at the tip and the nearly u_0 conditions at the shoulder of the cone indicates that peat behaviour around the cone is partly drained. Boylan et al. (2011) also report partly drained behaviour of peat during CPTU testing for some Dutch peats.

5 LABORATORY TESTING

An extended laboratory testing programme is part of this study. This section focuses two phenomena observed in the laboratory tests, that are considered typical for peat behaviour. As part of the testing programme 8 K_0-Constant Rate of Strain tests, K_0-CRS test were conducted on peat and 3 on samples from the clay layer below the peat. The K_0-CRS test is Constant rate of Strain test that has the option to measure the lateral stress during the test. Lateral stress measurement can be used in analyzing the data in e.g. the $p' - q$ space allowing assessment of parameters required for sophisticated material models in finite element codes, see Den Haan & Kamao (2003). The lateral stress measurement also allows for the assessment of K_0 during the test. In this study, besides the K_0 and parameters for finite element modeling, the K_0-CRS tests are used to support the classical oedometer tests. Figure 10 shows the test results, using natural strain, ε^H. With ε^C representing the linear strain, ε^H is defined by:

$$\varepsilon^H = -\ln\left(1-\varepsilon^C\right) \tag{3}$$

The stress – strain curve, Figure 10b, shows the applied loading paths includes an unloading – reloading loop, a phase of constant sample height and unloading at the end of the test. The phase with constant sample height is applied for the assessment of creep parameters.

The Figure 10a shows the K_0 measurement. Initially high values for K_0 are found. This is explained by inaccuracies in placing the sample in the ring and overconsolidated behaviour of the sample before the yield stress is reached. At larger strain levels the normally consolidated state is reached. At this stage $K_0 = K_{0,nc}$. Comparison of Figure 10a and 10b shows that $K_{0,nc}$ conditions are reached at larger strain levels, $\varepsilon^H = 0.6$ to 0.8, then obtained when reaching the pre-consolidation stress, $\varepsilon^H < 0.2$

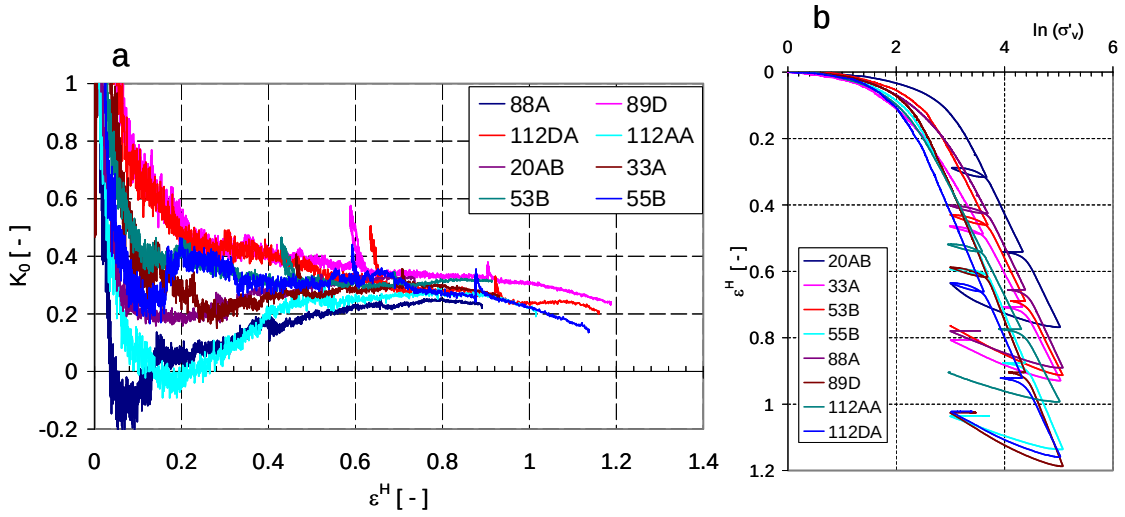

Figure 10. Results of the K_0-CRS tests on peat

Table 1. Summary of $K_{0,nc}$ values

sample	depth [NAP m]	W [-]	K_0 [- [
112AA	-4.47	10.1	0.24
112DA	-5.07	11.3	0.27
20AB	-2.34	8.7	0.27
33A	-4.08	7.6	0.28
53B	-2.45	9.6	0.30

55B	-4.53	10.8	0.27
88A	-3.49	10.2	0.22
89D	-5.11	11.0	0.32

Table 1 summarizes the $K_{0,nc}$ values found in Figure 10. On average is found $K_{0,nc}$ = 0.27. This is a low value compared to other materials, e.g. for the clay below the peat layer is found $K_{0,nc}$ = 0.5. A low $K_{0,nc}$ is typical for peat, Den Haan & Kruse (2007) and is explained by the fibre reinforcement.

Part of the laboratory testing programme are 5 anisotropically consolidated triaxial compression tests in which the vertical consolidation stress is chosen equal to the estimated vertical effective stress in the field. The horizontal consolidation stress is chosen according to the $K_{0\,nc}$ values presented by Table 1. As a consequence of this low value, in a *p'- q* diagram the $K_{0,nc}$ line lays relatively close to the failure line. In the followed consolidation procedure first the isotropic stress is applied followed by the deviatoric stress component.

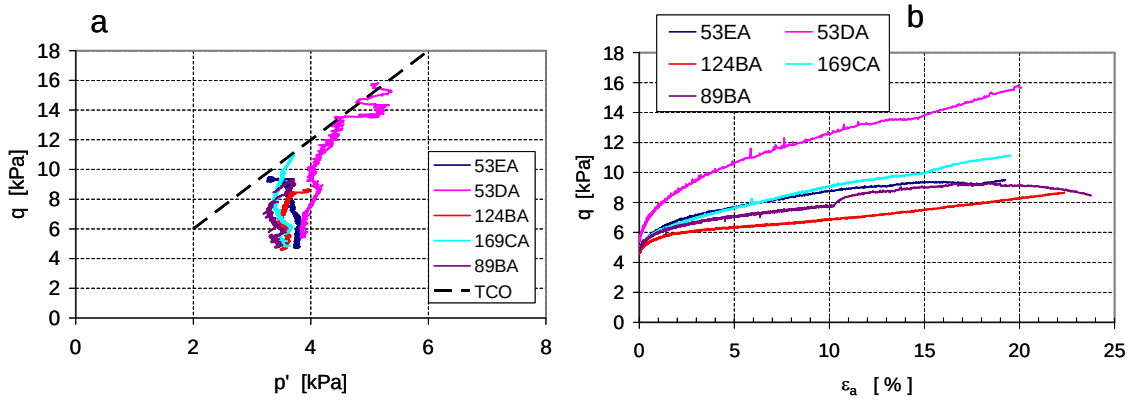

Figure 11. Results of anistropically consolidated triaxial compression tests a) *p'- q* diagram b) stress strain curve, TCO = Tension Cut Off line, ε_a = vertical strain

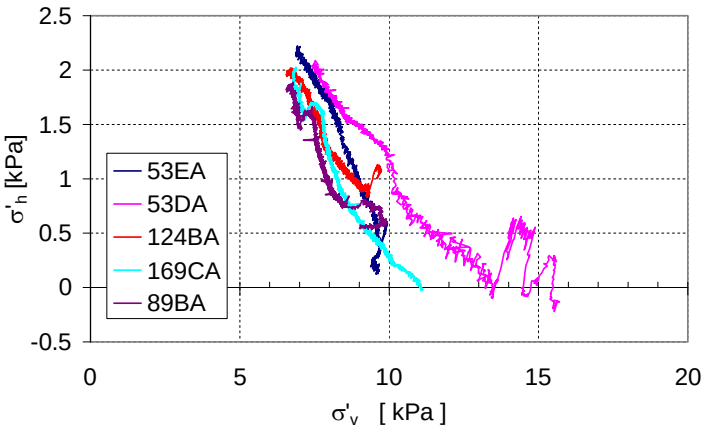

Figure 12. Results of anistropically consolidated triaxial compression tests during undrained loading phase, development of horizontal and vertical effective stress.

Figure 11 shows the stress curves and stress – strain curves for the five tests. The stress – strain curves, Figure 11b, show no clear peak. Increasing strain leads to an increase in mobilized shear strength even at high strain levels and failure is not easily identified. The stress paths, Figure 11a, end on or near the tension cut off, TCO, line. This state is reached when pore pressure inside the sample increases, in the undrained compression phase of the test, until the pore pressure equals the applied cell pressure. Then, the effective horizontal stress reduces to zero and there is no effective lateral support on the sample. Figure 12 shows the reduction in horizontal effective stress during the undrained compression phase. This is typical behaviour found in triaxial compression tests on peat, see among others Yamagutchi (1985), Den Haan & Kruse (2007), Zwanenburg et al (2012). Most of the tests discussed by these authors

are normally consolidated tests on peat in which during the undrained compression phase the stress paths reach the TCO-line. Since for TCO conditions no effective lateral support is acting on the sample, storage of pore water between the sample and membrane leads to drained conditions. Further loading causes the stress path to follow the TCO-line. The stress paths shown by Figure 11 stop when reaching the TCO line. The vertical strain, applied in the tests presented by Figure 11, corresponds to the test results reported by the authors mentioned above. Apparently, when consolidated at field conditions, more deformation is required, to generate the pore pressure increase needed to reach the TCO line. This will be studied in further laboratory testing.

6 FIELD TESTS

The first test was executed during October 19th to 22nd 2011 and was followed by the second test from 26th to 29th October 2011. The two tests are conducted nearly identical. Table 2 shows the order of events during the tests in which $t = 0$ relates to the start of the individual tests. The reported test phases are shown by Figure 1. Initially, an excavation depth of ground level -3.5 m was planned. However, in test 1 uplift of the excavation bottom occurred at a depth of approximately ground level -3 m. In further testing the excavation depth was restricted to ground level – 2.5 m.

Table 2. Following order of events during the test related to the start of each test

description	test phase	Time since start test 1 [hours]	Time since start test 2 [hours]
Start test	1	0	0
Start stepwise excavation	1	1:11	1:20
Finish stepwise excavation	1	14:11	17:45
1st step filling container, 0.25 m	2	27:11-28:11	27:04
2nd step filling container, 0.5 m	2	29:15-29:47	29:49-30:05
3rd step filling container, 0.75 m	2	31:24-31:42	34:00-34:18
4th step filling container, 1.00 m	2	33:54-34:19	41:53-42:19
5th step filling container, 1.25 m	2	39:01-39:29	45:45-46:06
6th step filling container, 1.50 m	2	44:35-45:01	51:32-51:50
7th step filling container, 1.75 m	2	51:34-52:00	57:06-57:23
1st step lowering water table, -0.25 m	3	53:06-53:45	57:06-57:23
2nd step lowering water table, max	3	54:34-57:	58:33-59:52
failure	3	55:42-55:54	59:00
extra step filling container test 2, 2.00 m	3	-	61:12-62:42

Figure 13 to 15 give a summary of the measurements. Figure 13 shows the vertical displacements and the filling of the containers. During excavation, phase 1, the vertical displacements are small. In phase 2, each loading step gives an initial acceleration of the vertical displacement, which gradually slows down until the next step gives a new acceleration. In later filling steps, vertical displacement reacts more strongly then in the initial loading steps. In both tests, the displacement reacts strongly to lowering the water table, phase 3.

Figure 14 shows the hydraulic head measurements during the tests in the middle section, see figure 3. The hydraulic heads are measured by Vibrated Wire Piezometers, that are pushed in position by a CPT rig. The piezometers have an accuracy of 0.3 kPa, which is equivalent to a hydraulic head (change) of 0.03 m. It should be noted that the presented measurements are not corrected for the vertical displacement of the monitoring equipment. Since the depth of the equipment could only be established before and after the test. Most of the vertical displacement develops at the end of test, near failure. So, corrections for the other test stages are small. During excavation, phase 1, a minor reduction in hydraulic head is measured. The hydraulic head measurements react clearly to the different loading steps in phase 2. During the test escaping gas bubbles were observed regularly. Collection of gas around the probes might explain the less sharp hydraulic head reaction to the loading steps at the end of the test. At failure,

some measurements show a sudden sharp decline in hydraulic head. Most measurements do not indicate failure. Also, a gradual increase in hydraulic head, indicating plastic behaviour of the sub soil is not found.

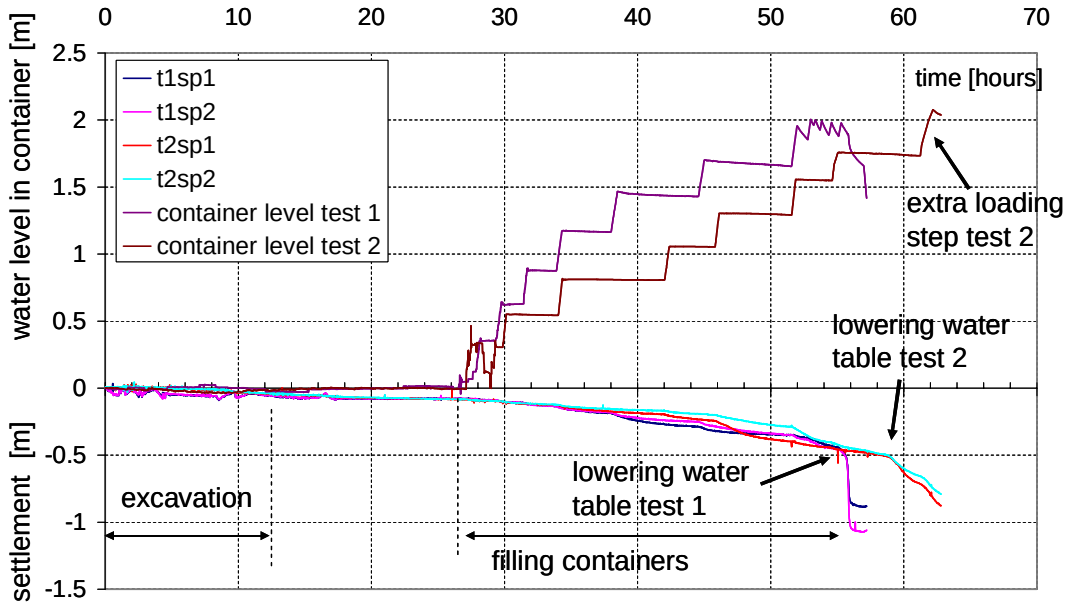

Figure 13. Vertical displacement measurements

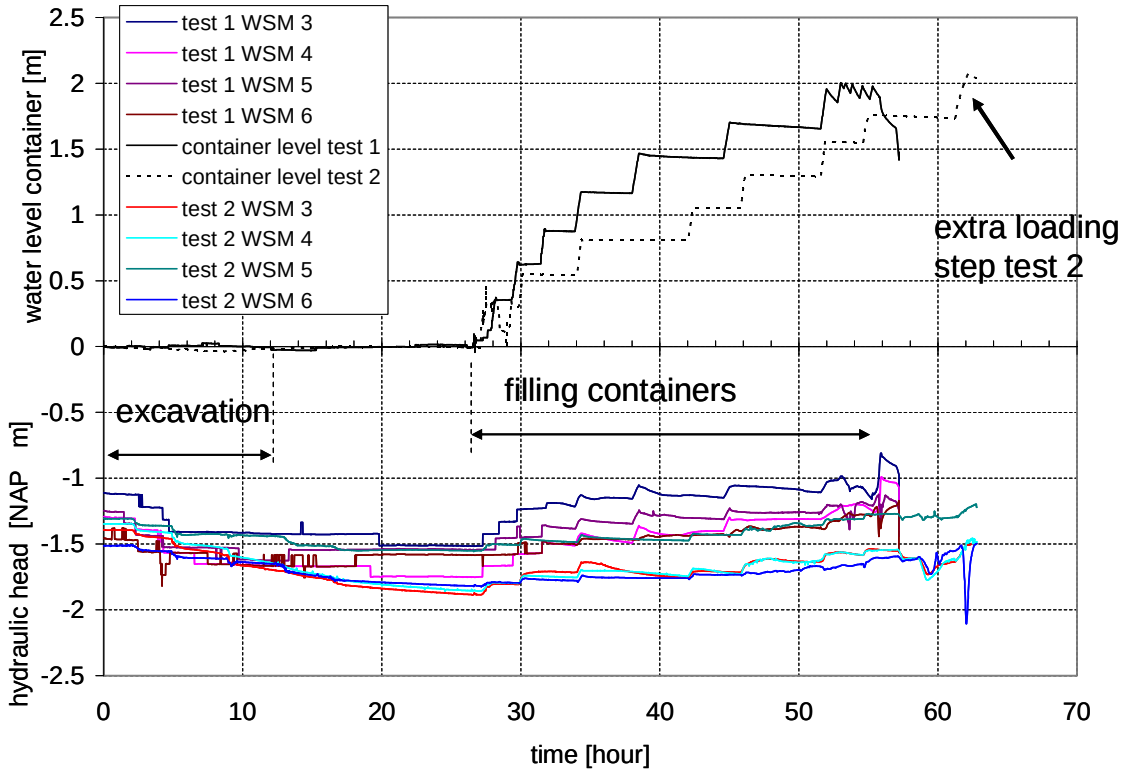

Figure 14. Hydraulic head measurements in middle section

Figure 15a and 15c show the final distribution of the horizontal displacements along the depth for test 1 and 2. For the middle section in test 1 relatively large horizontal displacement is measured in the clay and sand layer below the peat layer. These deformations developed only during failure. It is unlikely that at these levels displacements were found. Probably, at failure, the measurement device displaces such that unrealistic deformations were found. The maximum horizontal displacement was found in the range NAP -4.35 to -3.64 m, which is near excavation depth, NAP -3.9 m (2.5 m below ground level).

Figure 15b and 15c show the development of the horizontal displacements during the test at the depth of the maximum horizontal displacements at failure. During the excavation, the horizontal displacements remain relatively small. Although it should be noted that in early stages the maximum horizontal displacement develops at a higher level. Each step in filling the containers causes acceleration in horizontal displacements. Failure of test 1 is clearly identified in Figure 15b. While in test 2, Figure 15b, the horizontal displacements develop more gradually.

Test 1 and 2 are conducted nearly identical. Figures 13 to 15 show that displacements and hydraulic heads develop nearly equivalent. So it is concluded that the test results are reproducible. The most important difference in test result is found at failure, when test 1 shows a rapid displacement increase while test 2 shows a more gradual development.

After finishing the test a small field survey including two ball penetrometer tests, was conducted. Figures 16 gives the results for test 1. Equivalent results were found for test 2. The graphes clearly show the ground level to be lowered by approximately 0.8 to 0.9 m during the test. This settlement corresponds to the measured settlement during the test. It is remarkable that below the top layer, at approximately NAP -2.7 m, no change in measured resistance is found. Only in the top layer some strength increase is found. At the depth of NAP – 3.4 m and NAP – 3.7 m a reduction in measured resistance is found. This reduction corresponds to the location of the horizontal rupture planes.

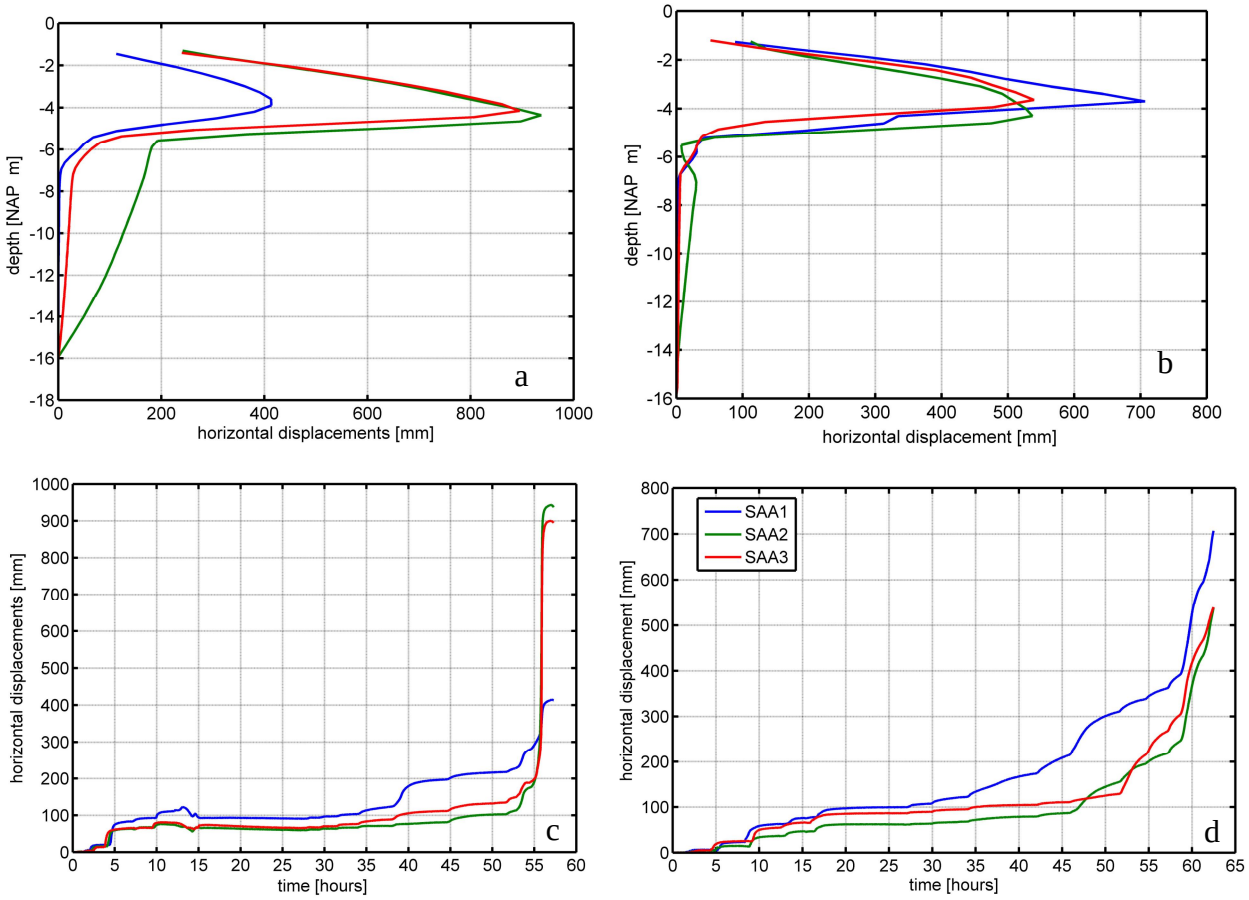

Figure 15. Horizontal displacements a) final distribution of horizontal displacements test 1 b) development of horizontal displacement in time test 1 at depth of final max. displacement c) final distribution of horizontal displacements test 2 d) development of horizontal displacement in time test 2 at depth of final max. displacement

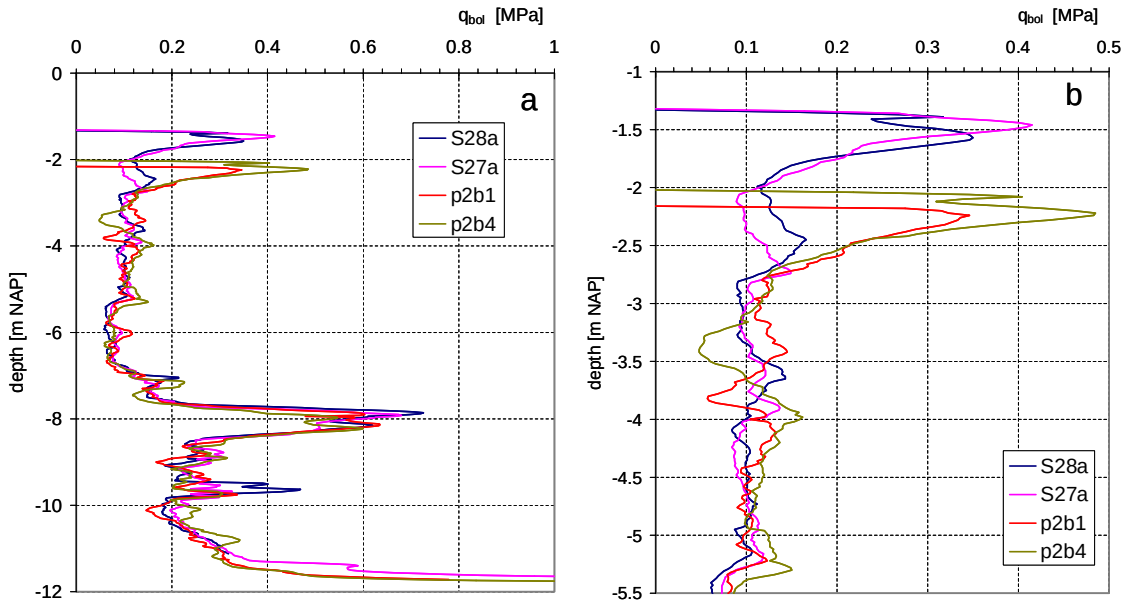

Figure 16. Comparison of ball penetrometer tests before and after test 1. a) complete measurement b) zoomed in on peat layer.

7 FAILURE MECHANISM

Section 6 concludes that the tests showed reproducible results, except for deformation rate near failure. In contrast to test 1, deformation developed more gradually in test 2, no progressive failure was found. During both tests, the containers tilted and leaned backwards, away from the excavation, at the end of the test. Continuous overtopping of water from inside the container, shown by Figure 17 indicated failure. At the active side a large vertical displacement was observed, see Figure 17. At the passive side, the excavated slope, only minor bulging was observed.

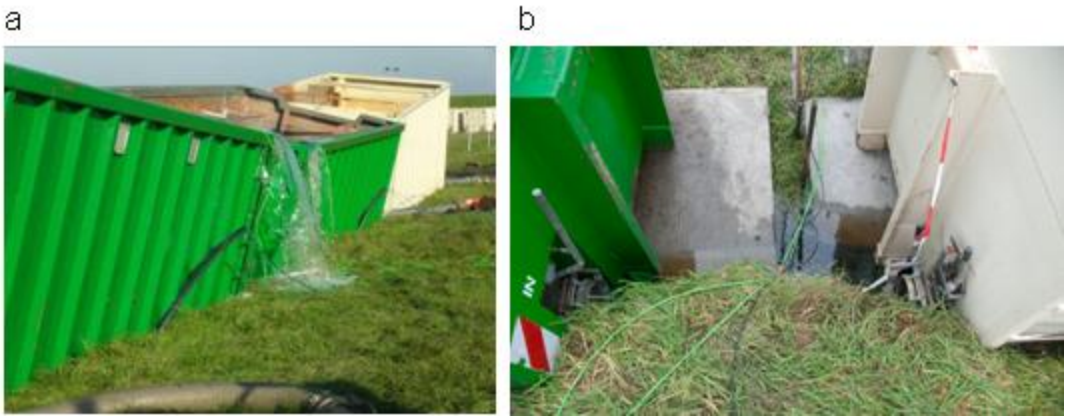

Figure 17. Sub soil failure a) overtopping of the containers due to excessive tilting in test 1, b) view on the active side of the failure.

Figure 18 shows the imprint of the containers after removal for both tests. The photo's clearly show the vertical deformation underneath the containers and the excavation slope being still intact. Figure 18 also shows the deformations being larger in the middle than at both ends of the removed container row. This indicates the influence of 3D effects. Due to extra resistance at the sides less deformation develops. For test 1, the difference in deformation at the middle and the ends of the container row seems larger then found in test 2. A small change in testing procedure might explain this difference. The containers were interconnected allowing the water to flow from one container to the other. This was advantageous in the

initial loading steps since the filling rate was different for the different containers. In this way an equivalent water level rise was implied in each container. For the final stages however the middle container settled more and therefore attracted water from the neighbouring containers. This led to slightly higher loads in the middle of the container row. For test 2 each container was filled with an equivalent amount of water at each step and the interconnection between the containers was closed off. This led to a better control of the loading

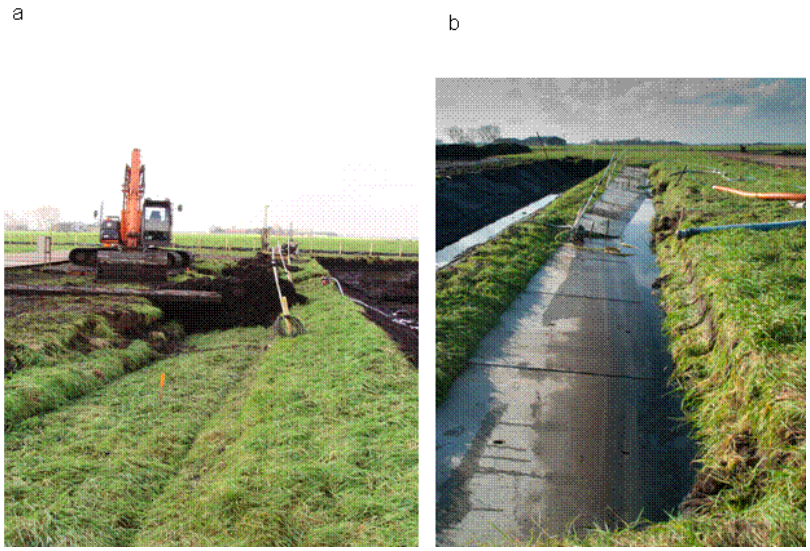

Figure 18. Container imprint found after removing the containers a) test 1 b) test 2

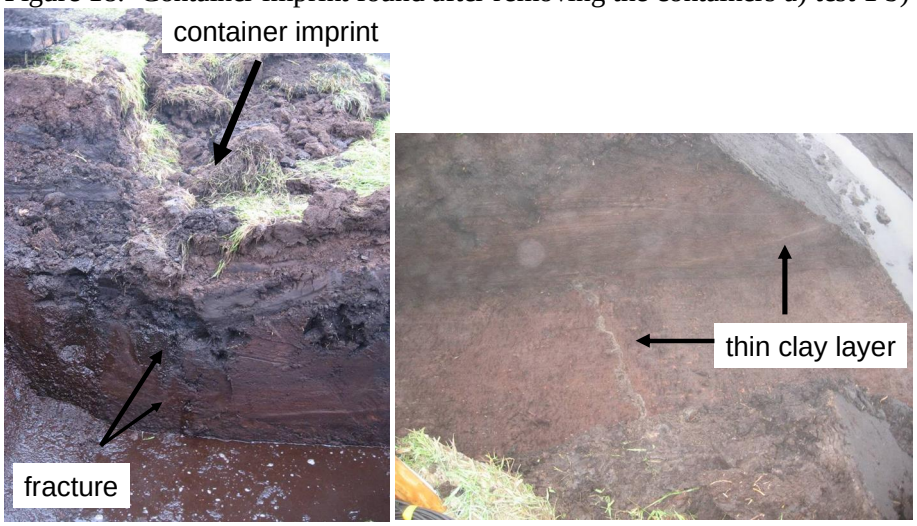

Figure 19. a) Vertical fracture found at the backside of the container imprint in test 2. b) Thin clay layer in peat deposit found in test 1.

After finishing the test, a trial pit, for inspection of the failure phenomena in the sub soil, was dug. In the sides and bottom of the trial pit several cracks with different orientations were found. It should be noted that the inspection was carried after removal of the containers. The removal of the containers causes unloading and therefore induces swelling of the peat layer. Cracks that originate from the failure in the test could not be distinguished from cracks caused by the unloading during removal of the containers. A clear rupture plane was found at the back side of the container. Displacements along-side this rupture plane coincides with the vertical displacements found at ground level up to a depth of 2 m. The face of the rupture plane is irregular and seems to bend around more stiffer and stronger parts in the peat layer. The width of the crack, after load removal, ranged between 5 to 50 mm. At the backside of the container secondary cracks were found, running away from the container, see Figure 20. The intersection with the main vertical crack showed that the secondary cracks originate from an early stage in the test, before the main vertical fracture was formed. These cracks might indicate a tendency for punching shear at an early stage of the test.

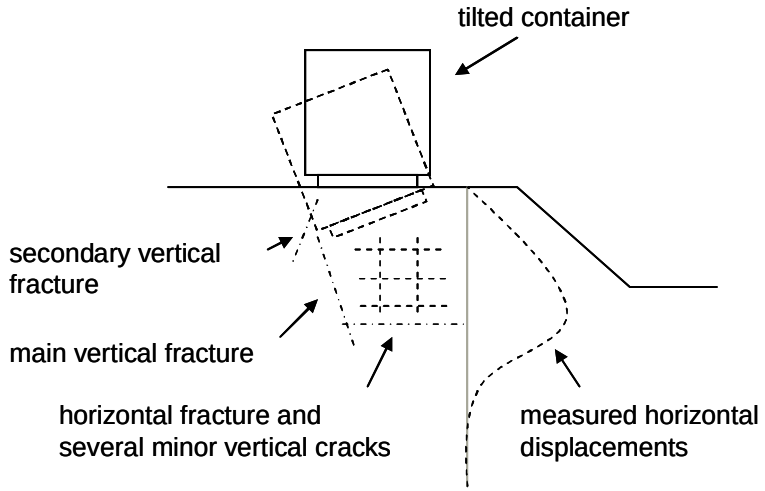

Figure 20. Sketch of failure mode

The main vertical rupture ends at a nearly horizontal crack. This crack lies at the level of maximum horizontal displacements measured by the SAA. The horizontal crack did not intersect the excavation. Inspection showed that no significant horizontal displacements occurred along the horizontal fractures. Above the main horizontal crack a number of horizontally and vertically oriented cracks were found with a mutual distance of 0.5 to 1 m. Some cracks were also found below the main horizontal crack. These cracks could originate from the rebound of the peat layer after the removal of the containers.

For test 1 a large vertical fracture was found nearly perpendicular to the container row. The fracture starts at the corner of a container and runs towards the excavation. Only one fracture of this type was found. However, it is to be expected that more of these fractures were present in test 1 and 2 but were not revealed by the trial pits.

The inspection showed the presence of old cracks filled with a few mm thick clay liner, see Figure 19b. This clay parting caused a considerable hydraulic resistance. A large increase in groundwater flow into the inspection pit was found when excavating through this layer.

Figure 20 summarizes the observed phenomena; a large vertical fracture coincides with an horizontal fracture. This horizontal fracture fades out and changes into compression of the peat. At the excavation, only some bulging of the excavated slope is found. Along the horizontal fracture, no sign of horizontal displacement was found. Besides the two main fractures several small horizontally and vertically oriented cracks were found underneath the container.

8 ANALYSIS

In engineering practice, regarding dike stability assessment, peat is considered firstly an undrained and secondly normally consolidated. This section compares these assumptions to the field measurements. Section 3 shows that the effective stresses are low, < 5 kPa. The pre-consolidation stress found in eodometer test ranges between 10 and 15 kPa, as shown by Figure 6. This implies an Over Consolidation Ratio, OCR > 2. For most civil engineering purposes, the applied loading exceeds the pre-consolidation stress easily and peat is usually considered as a normally consolidated material. In the tests however the load is relatively small. Due to stress distribution, the applied load increment decreases in depth. The maximum applied load during the tests, acting on the 2 m wide concrete slabs is 26 kPa, including the weight of the slabs. A stress distribution 2(v):1(h) results at the excavation depth, approximately ground level -2.5 m, in a load increment of approximately 6 kPa. Therefore, it is not likely that the normally consolidated state is reached during the test.

Leroueil et al (1990) discusses sub soil behaviour under an embankment during construction. Linear elasticity would predict a pore pressure increment equal to the isotropic stress increment. At the middle of the embankment, this increment equals the increment in vertical stress. Leroueil et al (1990) however shows that for many practical cases, initially, a lower response is found. This is explained by over

consolidated behaviour of the sub soil and an incomplete saturation of the top layer. When the vertical stress increment, $\Delta\sigma_v$ exceeds the pre-consolidation stress, the pore pressure reaction, Δu increases rapidly to $\Delta u = \Delta\sigma_v$.

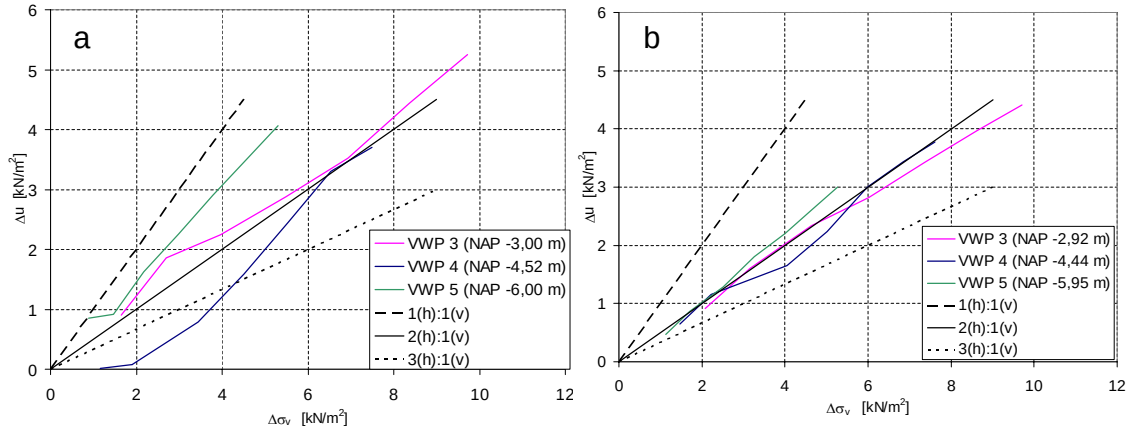

Figure 21. Measured pore pressure reaction, Δu versus vertical loading increment, $\Delta\sigma_v$ a) test 1, b) test 2

Figure 21 shows the pore pressure reaction as a function of the load increment found in the tests 1 and 2 in the middle row. The presented load increment $\Delta\sigma_v$ is corrected for stress distribution, 2(v):1(h). On average is found $\Delta u_2 = 0.5 \times \Delta\sigma_v$. It should be noted that the deformation and stress distribution is not one-dimensional, so a pore pressure response smaller then vertical load increment is to be expected. However, the bilinear behaviour described by Leroueil et al(1990) is not found in the measurements, indicating that during loading the stress level did not exceed the pre-consolidation stress.

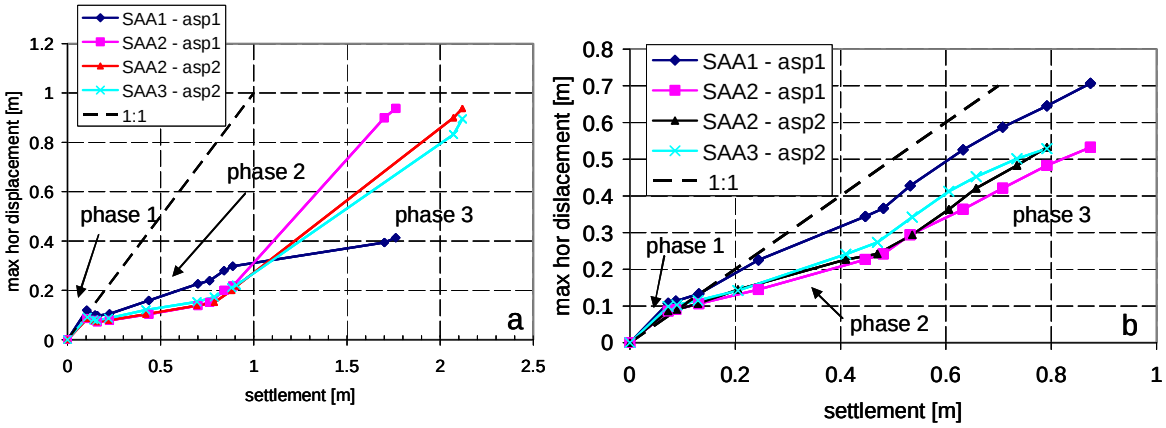

Figure 22. Maximum horizontal displacements versus settlement a) test 1, b) test 2

Figure 22 shows the relation between the vertical and horizontal displacements. The vertical displacements are measured by the automated settlement plates, located underneath containers 2 and 3, see Figure 3. During the test, the containers tilted backwards. The difference in settlement due to tilting at the end of the test was approximately 0.5 m in test 1 and 0.4 m in test 2. Since the automated settlement plates are located at the middle of the containers, the measurements are considered as the average value. The horizontal and vertical displacements are not measured at the same cross section as shown by Figure 3. The measured horizontal displacement, the maximum value for each selected test stage, is combined to the nearest automated settlement plate measurement. The measurements of horizontal displacements in the middle row, SAA2, are combined to both plates.

Figure 22 shows that during the excavation, phase 1, the horizontal displacement exceeds the vertical displacement. It should be noted that for test 1 during the period between finishing the excavation and the first loading step the horizontal deformation decreases. During loading, phase 2, the vertical displacement is larger then the horizontal displacement. For phase 3, the vertical and horizontal displacement are equal, the curves run parallel to the 1:1 line in Figure 21.

Leroueil et al (1990) discus measurements during the construction of three different embankments on soft soil. For each embankment, initially the vertical displacement was larger then the horizontal displacement. When loading continued and sub soil reached the normally consolidated state, it was found that the horizontal displacement increases strongly and for further loading the increments in settlement are equivalent to the increments in horizontal displacements.

Figure 22 shows that during phase 2, filling the containers the settlement underneath the containers exceeds the horizontal displacement. This corresponds to the observation that the maximum load does not exceed the pre-consolidation stress and that the pore pressure reaction does not indicate yielding. As soon as the lowering of the water table in the excavation starts the horizontal displacements increase such that further increments equal the increments in settlement. According to Leroueil et al (1990) this indicates yielding of the sub soil. As explained in the previous section, this stage resulted in large deformations and failure of the subsoil.

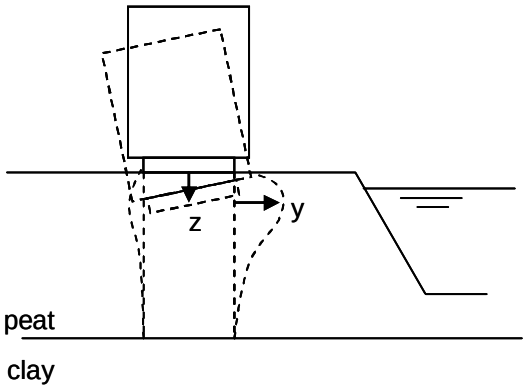

Figure 23. Vertical and horizontal displacements

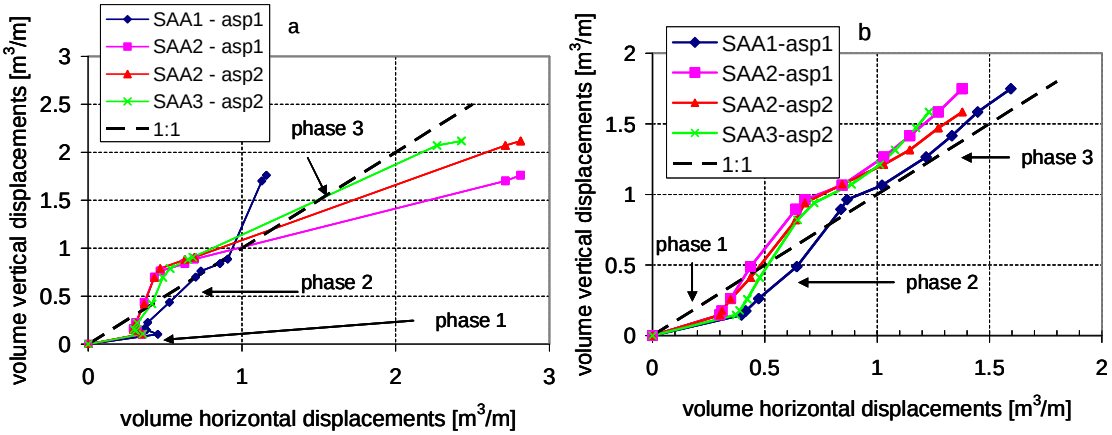

Figure 24. Volume change due to vertical versus horizontal displacements a) test 1, b) test 2

A further understanding in the behaviour of the peat layer underneath the containers is found by analyzing the volume change of the peat directly below the containers. Figure 23 sketches an element in the peat layer directly below the container by dotted lines. Undrained behaviour is characterized as constant volume behaviour. In Figure 23 volume is lost due to vertical deformation and volume is gained by bulging at the excavation side. The vertical displacement is measured at the middle of the concrete slabs providing the average vertical displacement of the backward leaning containers. Together with the width of the concrete slab, 2 m, and the assumption of plain strain conditions, the volume lost due to settlement is found, [m^3/m]. The horizontal displacements are only measured at the excavation side, see Figure 3. Landva (2007) shows that bulging, when peat is loaded perpendicular to the fiber orientation is negligible. Assuming horizontal fiber direction, gives negligible horizontal displacements next to the container at the opposite side of the excavation. An indication that this assumption might be true is found in the nearly vertical sliding at the backside of the container and no visual indication of horizontal deformation was found in the trial pit dug after the test was completed. For the next tests extra horizontal deformation measurements are planned at the backside of the containers. Under the assumption that the

horizontal deformations at the backside of the container row is negligible, the volume per m length, gained by bulging, is found by integration of the measured horizontal displacements along the depth.

Figure 24 shows the relation between horizontal and vertical volume change. Both are indicated by positive values, although vertical displacement leads to a volume loss and horizontal displacement to a volume increase. During excavation, the increase in volume in horizontal direction exceeds the decrease in volume in vertical direction. The total volume increases and the peat layer expands which (partly) explains the reduction in measured hydraulic head during excavation. It should be noted that the influx of groundwater to the excavation was limited during test 2. For test 1, the influx was low until uplift of the excavation bottom occurred. In phase 2, filling the containers, the volume lost due to vertical displacements exceeds the volume gained in horizontal direction. The peat underneath the containers compacts. In phase 3, lowering the water table, the volume gained in horizontal direction increases considerably. For test 2 the increase in horizontal volume balances the vertical volume loss indicating constant volume behaviour. For test 1, the horizontal increase in volume seems to exceed the loss in volume in vertical direction.

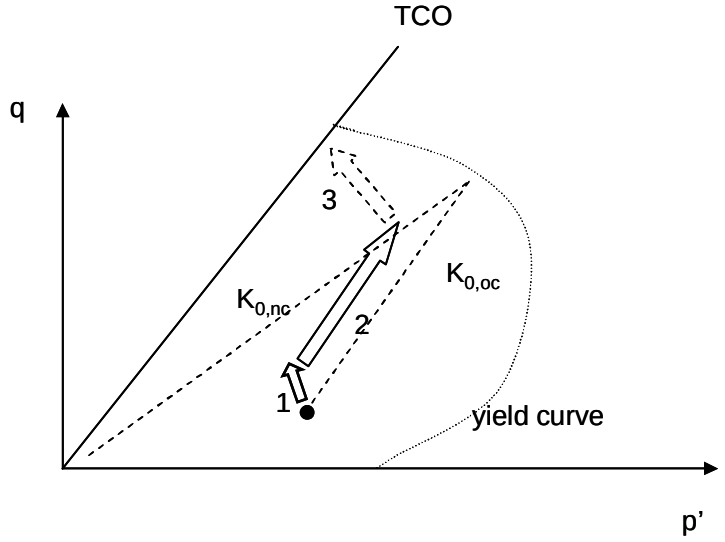

Figure 25. Sketch of stress path during test, the numbers correspond to the different phases in the test.

Figure 25 sketches the stress path for some point in the middle of block of peat indicated in Figure 23. It should be noted that the horizontal stresses are not known so an exact stress path cannot be drawn. All stresses are low causing the stress paths to be closely to the origin of the *p'-q* diagram. The analysis, given above, shows that the peat is in an over-consolidated state. The ratio horizontal to vertical effective stress is given by K_{0oc} which is unknown. Section 5 discusses the K_0-CRS tests. The tested peat samples showed a K_{0nc}= 0.27. So, in Figure 24 the K_{0nc} - line lays closely to the failure line. Since, the triaxial tests on peat failed when reaching the Tension Cut Off line, the TCO line is depicted as failure line. The excavation in phase 1 leads to a reduction in lateral stress, leading to an increase in *q*. Depending on the rate of consolidation *p'* is constant or shows some reduction. Since the tests shows partly drained behaviour of the peat, a small reduction is assumed in Figure 25. In phase 2, filling the containers, the peat layer behaves partly drained, as concluded from Figure 21 and 22, stress paths will develop in the direction indicated by the arrow in Figure 25. In phase 3, lowering the water table leads again to a reduction in lateral stress and an increase in *q*. Depending on the amount of drainage this might lead to some reduction in ground water table underneath the container. Measurements show that this reduction is negligible and *p'* is assumed nearly constant in Figure 25. In phase 3 the effective stress path direction changes. Since at the end of phase 2 the stress condition was close to the normally consolidated state, which in its turn is close to the failure line, failure is reached rapidly. This explains that the stability in the tests are found sensitive to a reduction of the water table in the excavation.

9 CONCLUSIONS

This paper describes two field tests. Since the tests are part of a larger project, which is still in progress, the conclusions found so far can only be considered preliminary. The background of the tests lays in determination of strength parameters for peat required for stability assessment of existing dikes. The tests are conducted nearly identical and the test results are consistent indicating that the test results are reproducible.

The failure mechanism found in the tests does not resemble the circular or semi-circular sliding plane that are usually applied in stability assessment of dikes. Instead, a nearly vertical active plane is found. Along this plane, fracturing has taken place; visual inspection shows that fibers are broken. The vertical rupture plane intersects with a horizontal plane. This horizontal plane starts as a clear sliding plane but fades out when sliding transforms into compression of the peat.

At the passive side the peat compresses. No clear passive sliding plane was found. However, other cases of failure through peat layers do show passive sliding planes, see e.g. Van et al (2008), Zwanenburg et al (2012). In the tests described in this paper, the load increments were small. Larger load increments might have led to more momentum and therefore to a clear passive sliding plane.

Analysis of the measured deformation and pore pressures indicates that overconsolidated behaviour plays an important role. In daily engineering practice, peat behaviour is not considered as overconsolidated behaviour. In general, for many civil engineering applications, a load is applied onto the peat layer such that the normally consolidated state is reached quickly. However, in the stability assessment of existing dikes load increments are small. At the sea or river side the raise in water level might induce an (effective) stress increase in the dike or sub soil. This increase however is not accounted for in conventional limit equilibrium analyses. Hydraulic connection due to sand layers underneath the dike might even cause a stress reduction, Bauduin & Barends (1988), Van et al (2011). The fact that the peat layer acts as an over consolidated material has a strong influence on the strength characteristics and will be topic of further study.

Although peat is known for its heterogeneity, the CPTU and ball penetrometer test results are remarkably consistent. The ball penetrometer tests show less variation, making them more appropriate for parameter assessment. The CPTU measurements indicated partly drained behaviour of the peat. Also, during the loading stages of the test the peat reacted partly drained. This was not expected before hand since peat is usually considered as a low permeable material. The partly drained behaviour might be connected to the conclusion that the peat behaviour is considered over consolidated and will be part of further study.

Fracturing at the passive side is also found at the IJkdijk test, Zwanenburg et al (2012) and in the Irish peat slides Dykes (2008). Tensile strength of peat seems important in understanding failure of peat. Some researchers have studied the tensile strength of peat and peat fibers e.g. Landva(2007). However, application of tensile strength in engineering practice or even in stability assessment of dikes is rarely. Tensile strength and fracturing of peat will be an item in continuation of this study.

REFERENCES

Abdoun T., Bennet V., Dobry R., Koelewijn A.R., Thevanayagum S. (2010) Real-time monitoring of full-scale levee testing *in: International Conference on Physical Modelling in Geotechnics Springman, Laue & Seward (eds)* Taylor &Francis Group, London Volume II, p 1171-1176

Boylan N., Long M., Mathijssen F.A.J.M. (2011) In situ strength characterisation of peat and organic soil using full-flow penetrometers *Canadian Geotechnical Journal* 48:1085-1099

Bauduin Chr., M.,H.,L.,G., Barends F.B.J. (1988) Getijde-respons in grondwater onder Nederlandse dijken *H2O* (21):2-5

Den Haan E.J., Kruse G.A.M. (2007) Characterisation and engineering properties of Dutch peats *in: Characterisation and Engineering Proporties of Natural Soils, Tan, Phoon, Hight & Leroueil (eds)* Taylor & Francis Group London ISBN 978-0-415-42691-6

Den Haan E.J., Kamao S. (2003) Obtaining isotache parameters from a C.R.S. K0-oedometer *Soils and Foundations* 43 (4):203-214

Dykes A.P. (2008) Tensile strength of peat: laboratory measurement and role in Irish blanket bog failures *Landslides* 5:417-429

Landva O.A. (2007) Characterization of Escuminac peat and construction on peatland *in: Characterisation and Engineering properties of Natural Soils Tan, Phoon, Hight & Leroueil (eds)* Taylor & Francis Group London p. 2135-2191

Lehane B.M., Jardine R.J. (2003) Effects of long-term pre-loading on the performance of a footing on clay *Géotechnique* 53(8):689-695

Leroueil S., Magnan J-P., Tavenas F., Wood D.M. (transl) (1990) *Embankments on soft clays*, Ellis Horwood series in Civil Engineering Ellis Horwood, Chichester ISBN 0-13-275736-2

Lunne T., Robertson P.K., Powell J.J.M. (1997) *Cone penetration testing in geotechnical practice* Blackie Academic & Professional London ISBN 0 751 40393 8

Skempton A.W., Petley D.J. (1970) Ignition loss and other properties of peats and clays from Avonmouth , King's Lynn and Cranberry Moss, *Géotechnique* 20 (4):343-356

Van M.A., Sharp M.K., Zwanenburg C., Mosher R.L., van Esch J.M. (2008) Horizontal translational Failures of Levees due to Water Filled Gaps *Proc 6th International Conference on Case Histories in Geotechnical Engineering*, Arlington VA 7

Van M.A., Koelewijn A.R., Barends F.B.J (2011) Uplift phenomenon: model, validation and design *in: A feeling for soil and water Van, Den Haan & van Deen (eds)* Deltares select series volume 7, ISSN-1877-5608

Yamagutchi H., Ohira Y., Kogure K., Mori S (1985) Undrained shear characteristics of normally consolidated peat under triaxiaal compression and extension *Soils and Foundations* 25 (3):1-18

Zwanenburg C., Den Haan E.J., Kruse G.A.M., Koelewijn A.R. (2012) Failure of a trial embankment on peat in Booneschans, The Netherlands *Géotechnique* in print

NOTATION

a	cone factor, eq(2) [-]
K_0	ratio of horizontal and vertical effective stress, [-]
N	loss on ignition, [%]
NAP	reference datum, approximately mean sea level
u_0	in-situ pore pressure, [kPa]
u_1, u_2, u_3	pore pressure measured at different position along the cone, Figure 8, [kPa]
p'	isotropic effective stress, [kPa]
q	deviator stress, [kPa]
q_c	cone resistance, [MPa]
q_t	corrected cone resistance, eq (2), [MPa]
W	water content, [-]
ε_a	axial strain, [-]
ε^C	conventional engineering strain, [-]
ε^H	natural strain, eq (3), [-]
ρ	density, [t/m^3]
ρ_s	solid density, [kg/m^3]
σ_{vy}	pre-consolidation stress, [kN/m^2]
σ'_v, σ'_h	vertical, horizontal effective stress, [kN/m^2]

ACKNOWLEDGEMENTS

The author acknowledges the Dutch Ministry of Public Works, Rijkwaterstaat-Waterdienst and the water board, Hoogheemraadschap Hollands Noorderkwartier, for making the tests possible. Gerard Kruse, Deltares – Geo engineering, was in charge for the trail pit and the description of the failure mechanism. The tests would not have been successful without the help of many colleagues at Deltares, during the execution of the tests as well as in discussing the measurement results afterwards.